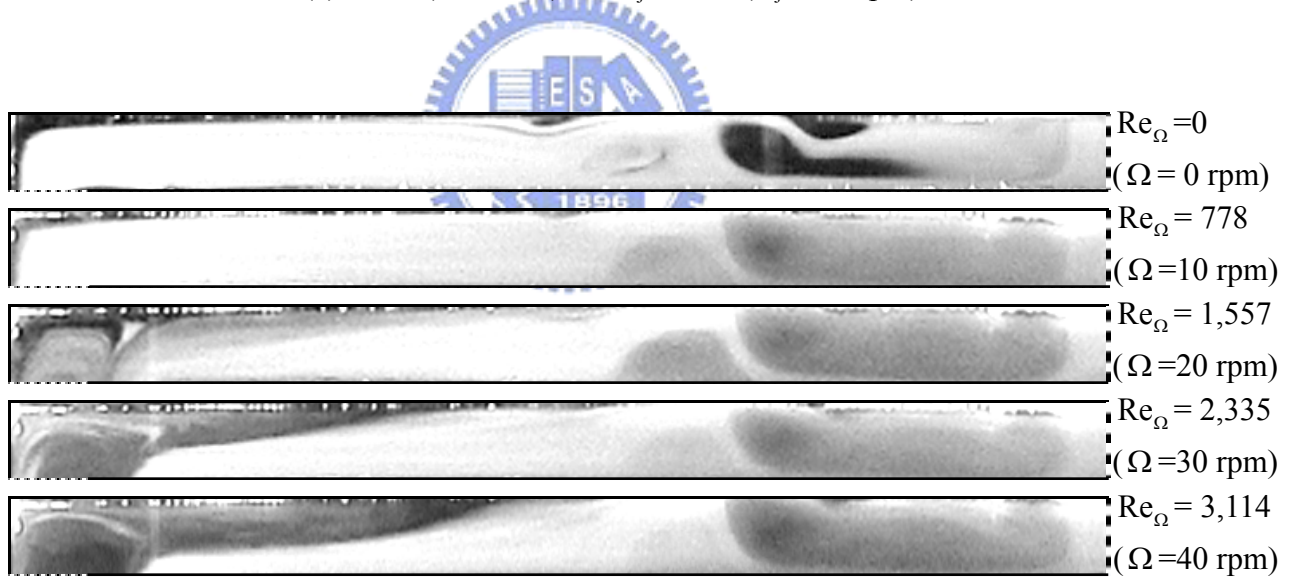


(a) $Ra=0$ ($\Delta T=0$) & $Re_j=1,150$ ($Q_j=8.5$ slpm)



(b) $Ra=470$ ($\Delta T=5.0$) & $Re_j=1,150$ ($Q_j=8.5$ slpm)

Fig. 4.18 Steady side view flow photos taken at the cross plane $\theta = 0^\circ$ for $Re_j=1,150$ ($Q_j=8.5$ slpm) for various rotational Reynolds numbers at $H=10.0$ mm for (a) $Ra=0$ ($\Delta T=0$) and (b) $Ra=470$ ($\Delta T=5.0$), (c) $Ra=940$ ($\Delta T=10.0$), (d) $Ra=1,410$ ($\Delta T=15.0$), and (e) $Ra=1,880$ ($\Delta T=20.0$).

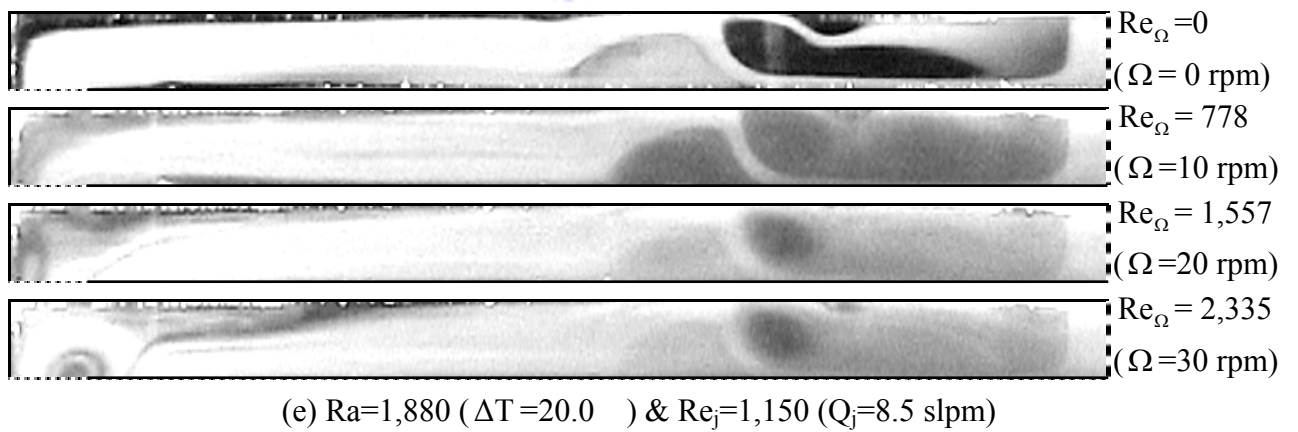
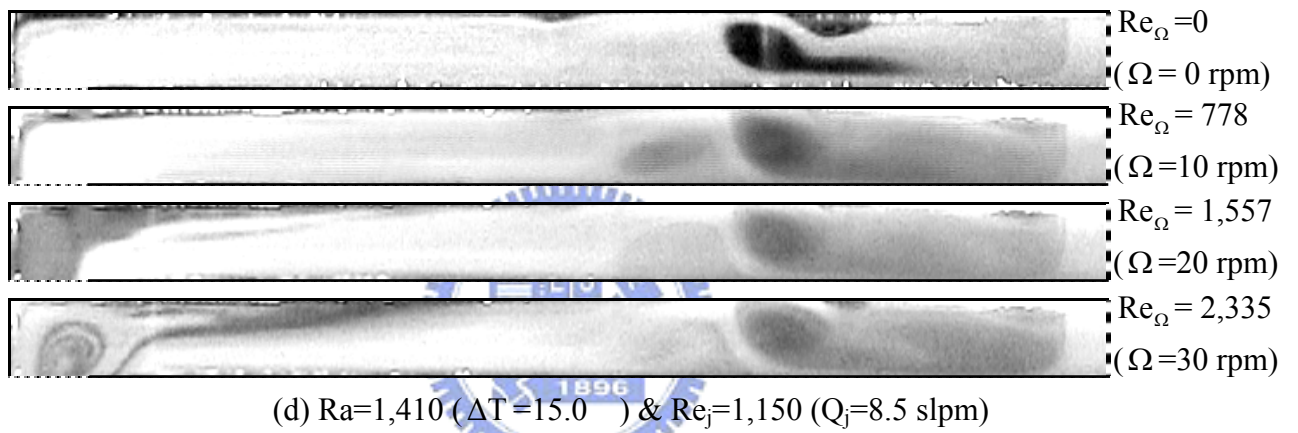
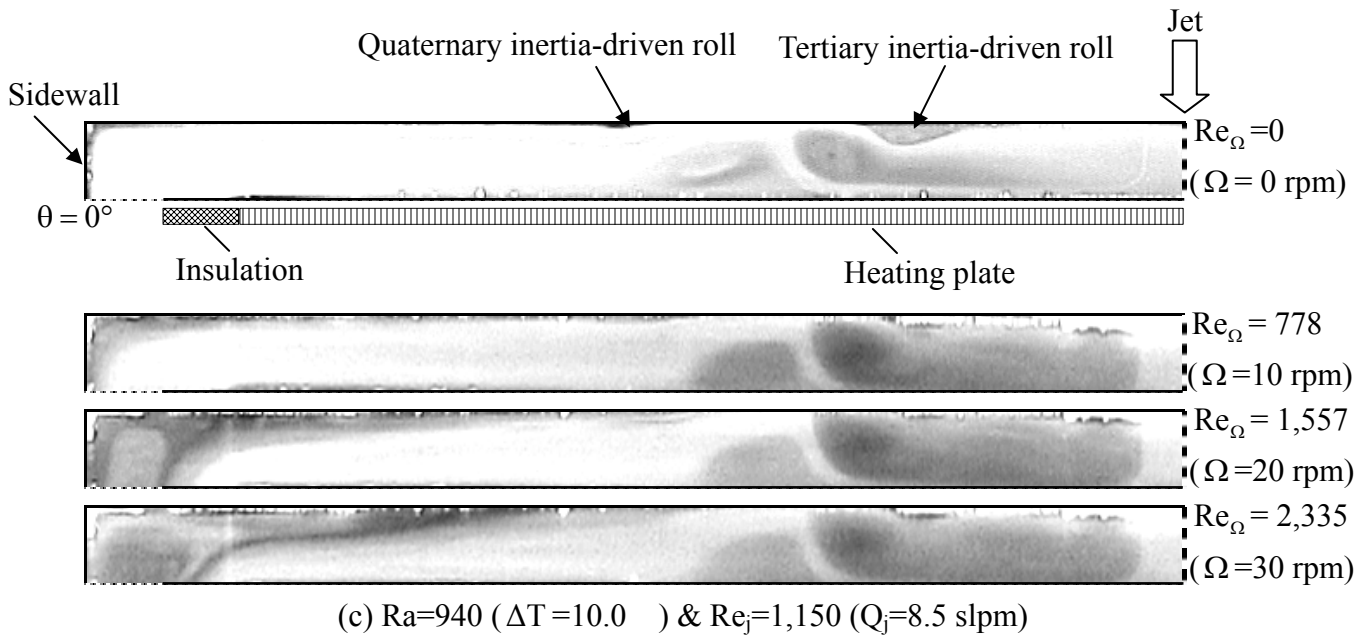


Fig. 4.18 Continued

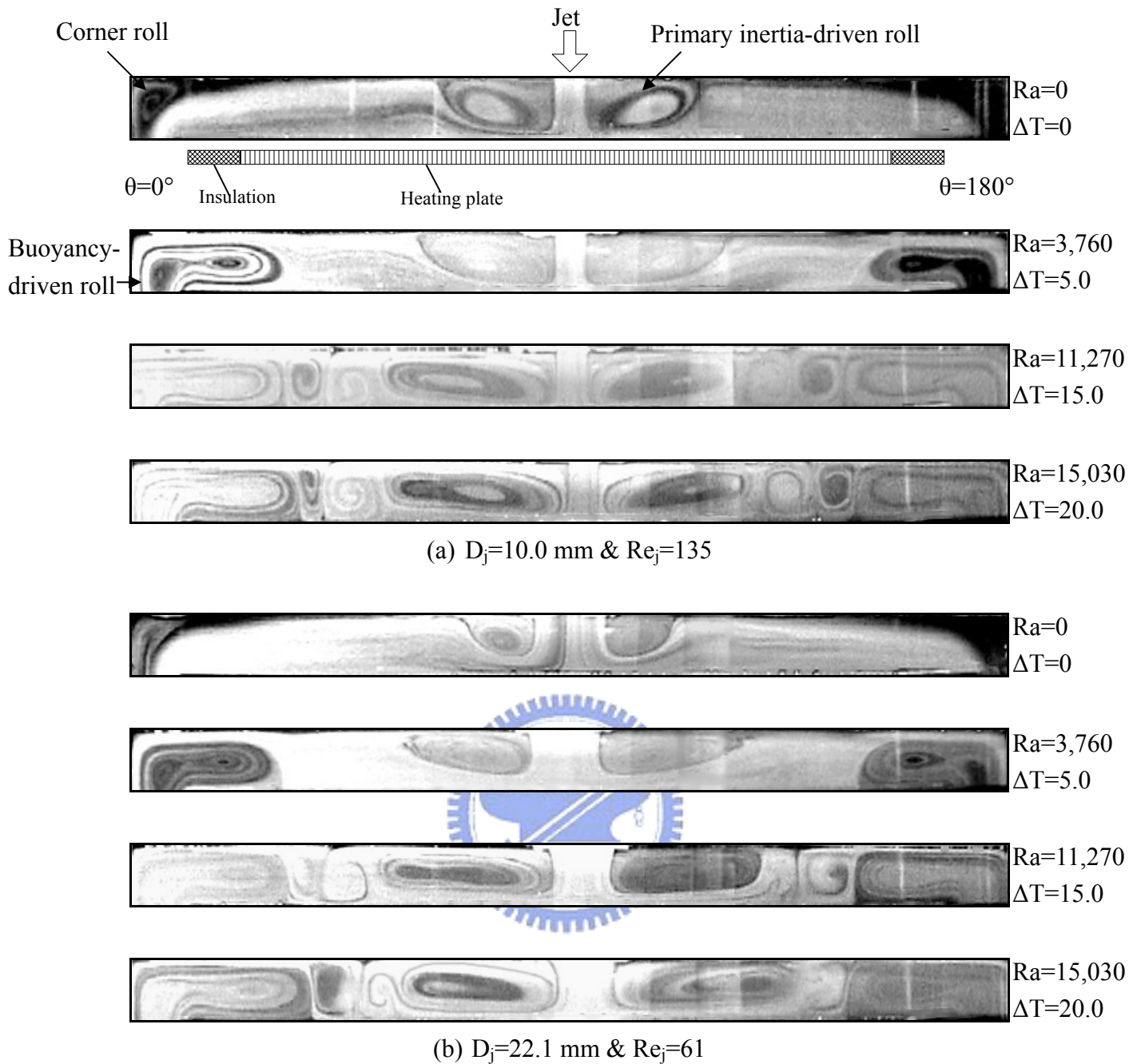


Fig. 4.19 Side view flow photos taken at the cross plane $\theta = 0^\circ$ & 180° for various Rayleigh numbers at $Q_j = 1.0$ slpm and $Re_\Omega = 0$ ($\Omega = 0$ rpm) for (a) $D_j = 10.0$ mm & $Re_j = 135$ and (b) $D_j = 22.1$ mm & $Re_j = 61$.

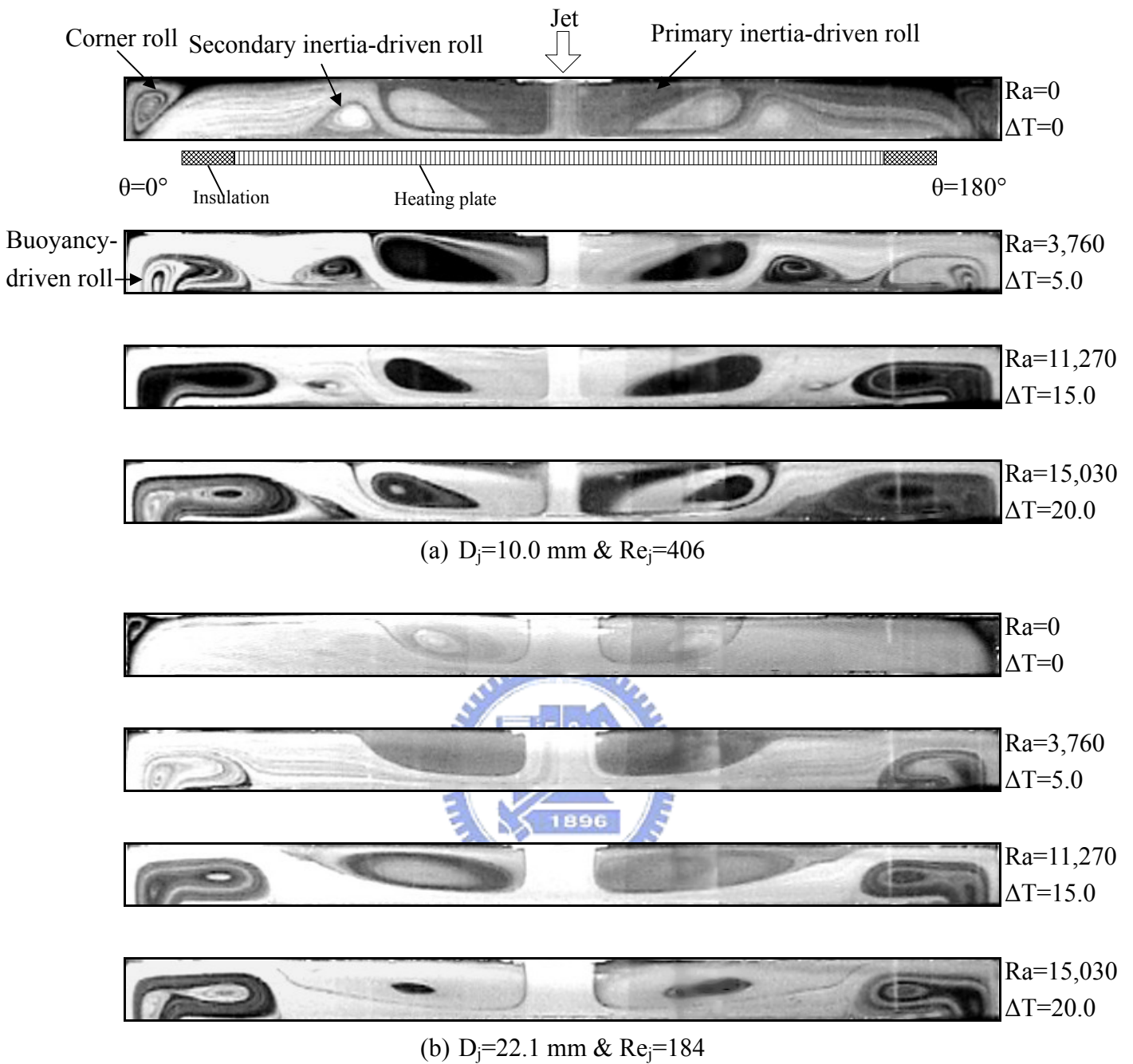


Fig. 4.20 Steady side view flow photos taken at the cross plane $\theta = 0^\circ$ & 180° for various Rayleigh numbers at $Q_j = 3.0 \text{ slpm}$ and $Re_\Omega = 0$ ($\Omega = 0 \text{ rpm}$) for (a) $D_j = 10.0 \text{ mm}$ & $Re_j = 406$ and (b) $D_j = 22.1 \text{ mm}$ & $Re_j = 184$.

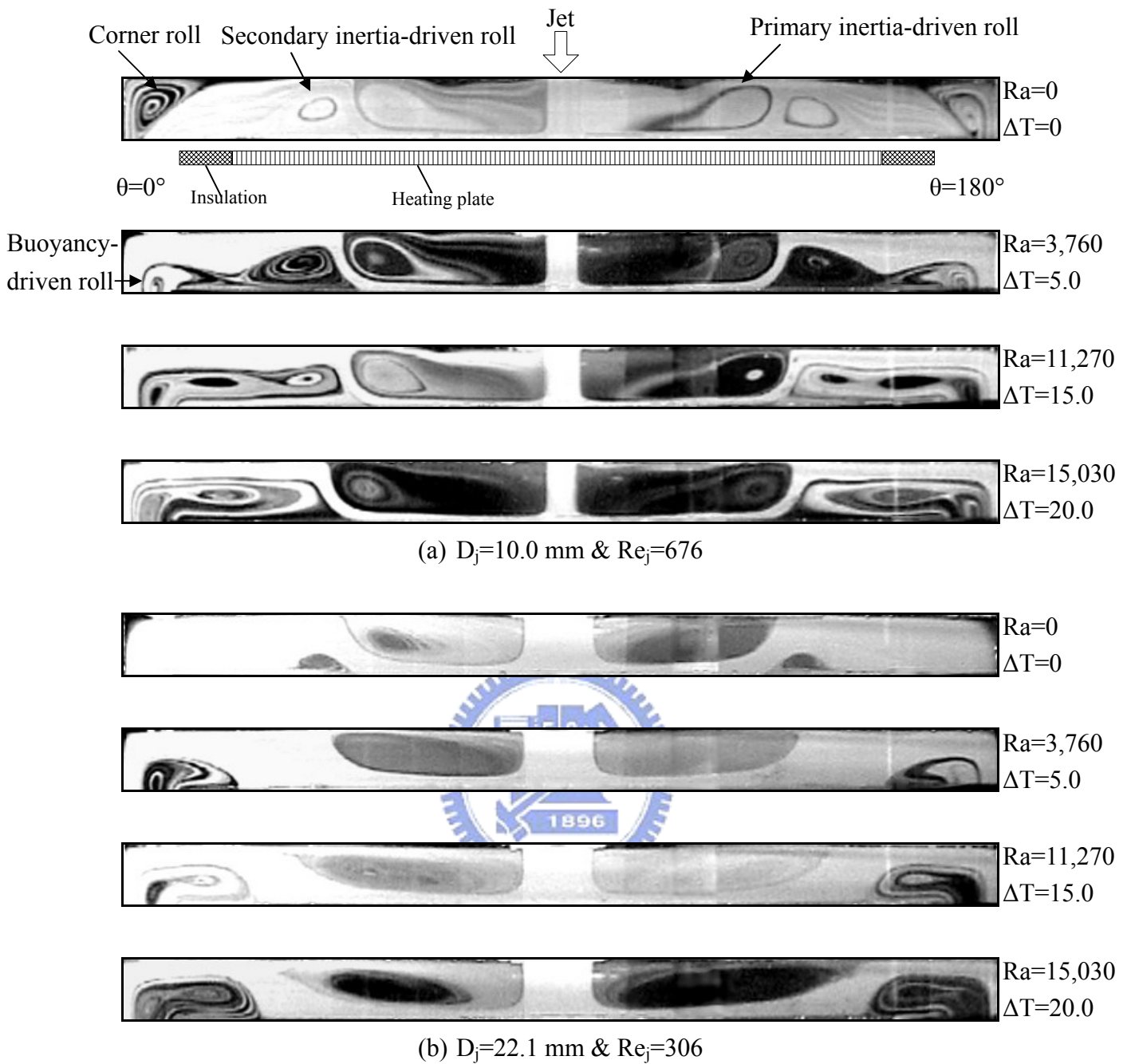


Fig. 4.21 Steady side view flow photos taken at the cross plane $\theta = 0^\circ$ & 180° for various Rayleigh numbers at $Q_j = 5.0$ slpm and $Re_\Omega = 0$ ($\Omega = 0$ rpm) for (a) $D_j = 10.0 \text{ mm}$ & $Re_j = 676$ and (b) $D_j = 22.1 \text{ mm}$ & $Re_j = 306$.

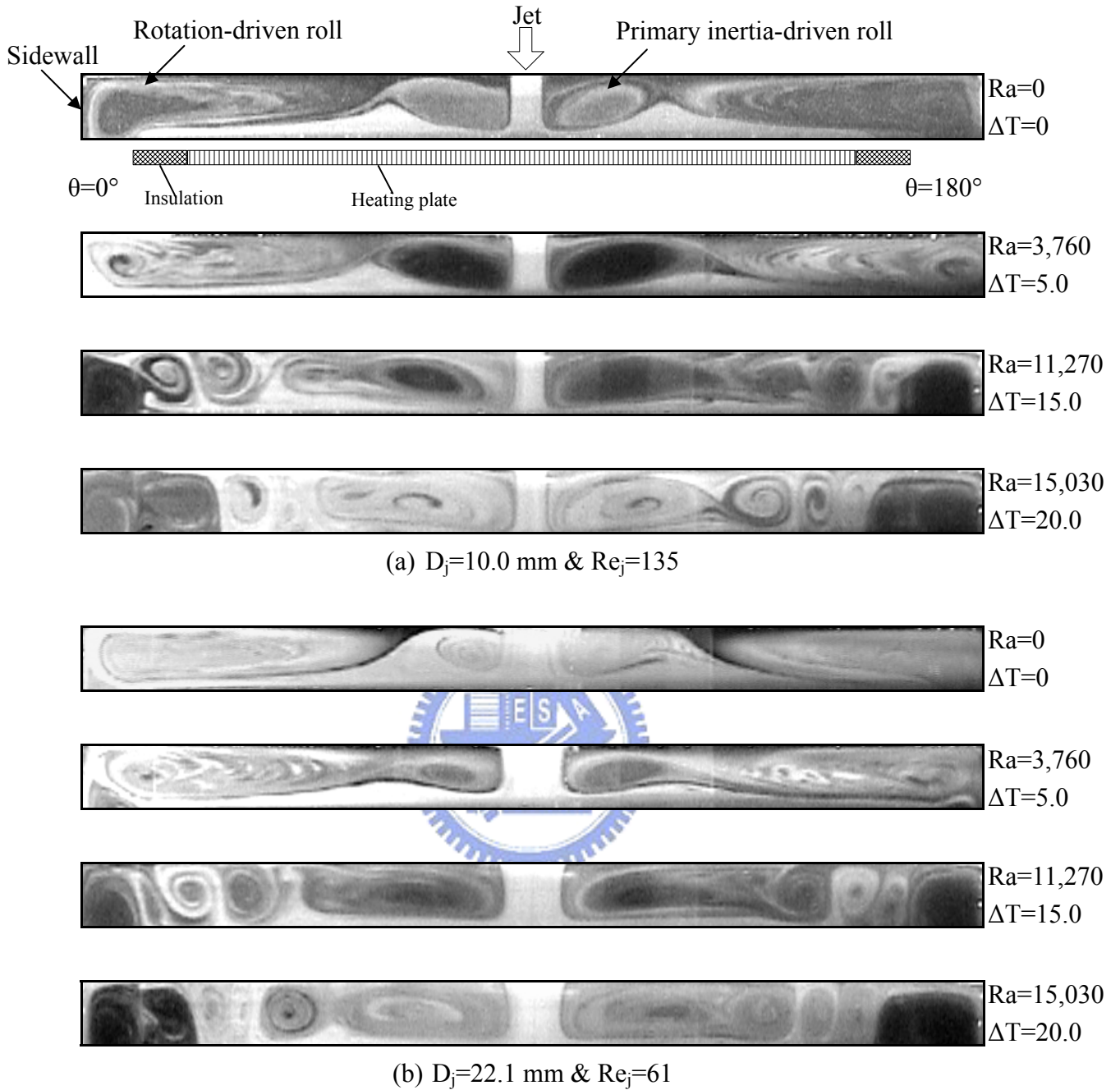


Fig. 4.22 Side view flow photos taken at the cross plane $\theta = 0^\circ$ & 180° for various Rayleigh numbers at $Q_j = 1.0$ slpm and $Re_\Omega = 778$ ($\Omega = 10$ rpm) for (a) $D_j = 10.0$ mm & $Re_j = 135$ and (b) $D_j = 22.1$ mm & $Re_j = 61$.

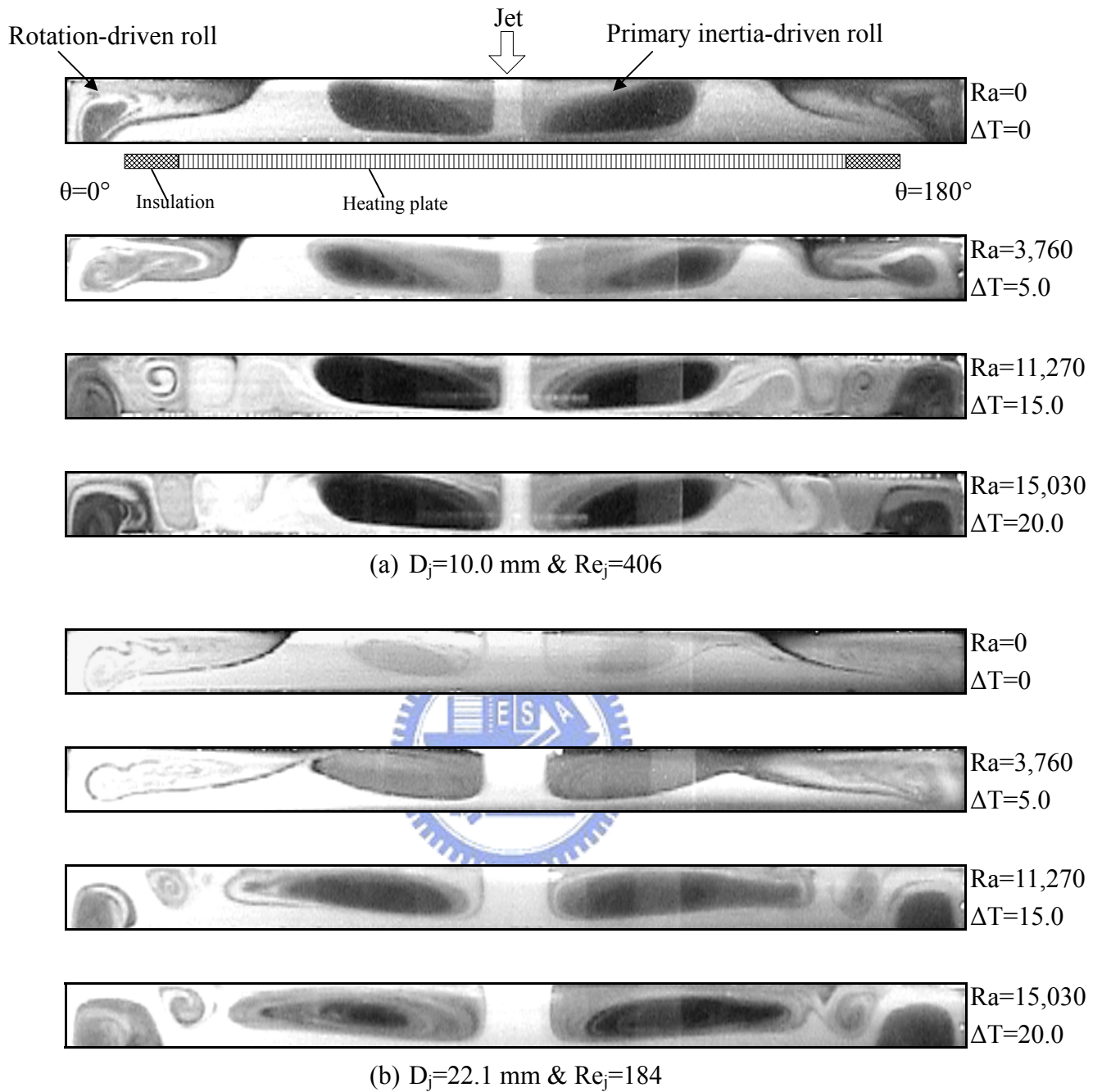


Fig. 4.23 Side view flow photos taken at the cross plane $\theta = 0^\circ$ & 180° for various Rayleigh numbers at $Q_j = 3.0 \text{ slpm}$ and $Re_\Omega = 778$ ($\Omega = 10 \text{ rpm}$) for (a) $D_j = 10.0 \text{ mm}$ & $Re_j = 406$ and (b) $D_j = 22.1 \text{ mm}$ & $Re_j = 184$.

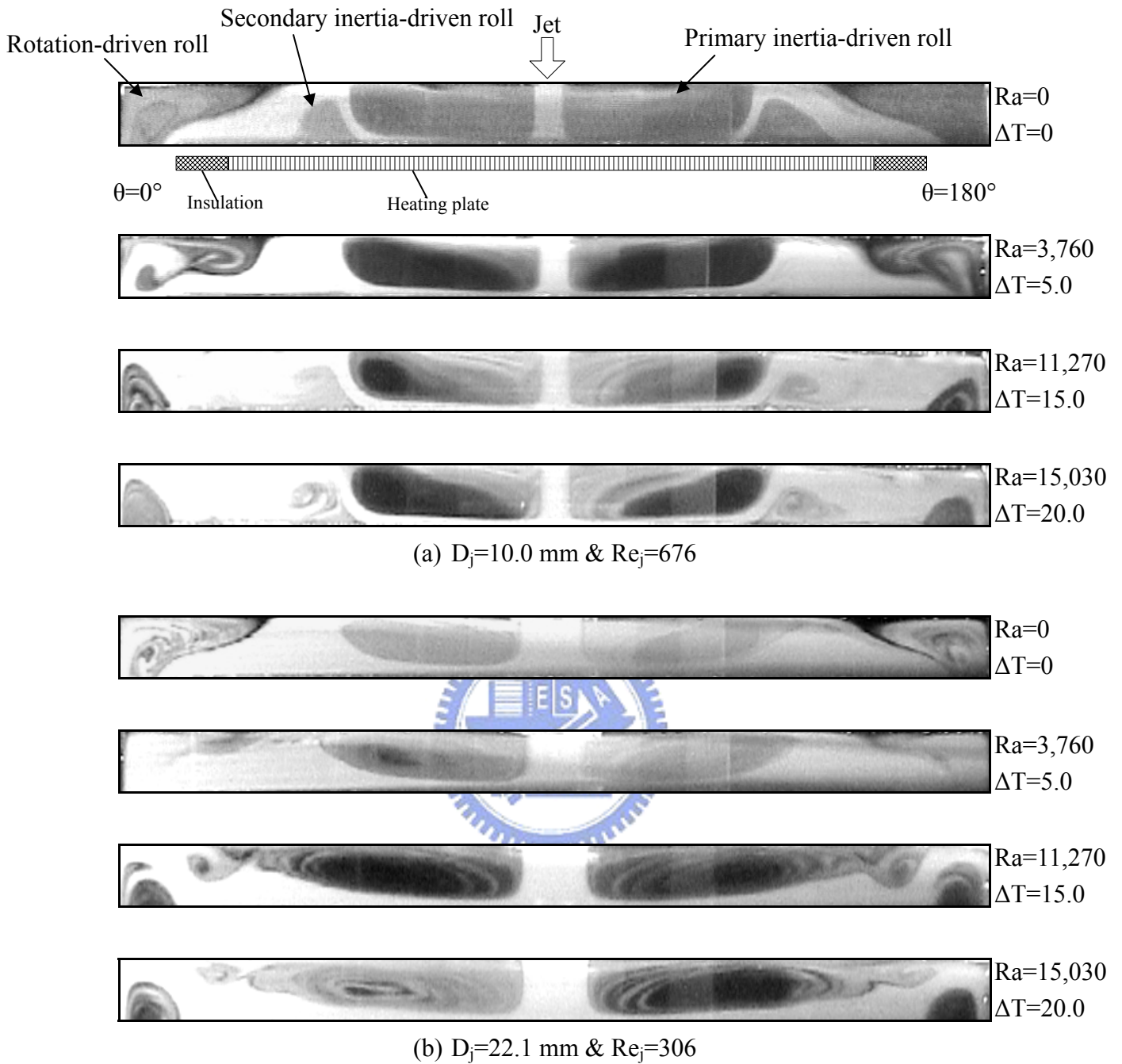


Fig. 4.24 Side view flow photos taken at the cross plane $\theta = 0^\circ$ & 180° for various Rayleigh numbers at $Q_j = 5.0$ slpm and $Re_\Omega = 778$ ($\Omega = 10$ rpm) for (a) $D_j = 10.0$ mm & $Re_j = 676$ and (b) $D_j = 22.1$ mm & $Re_j = 306$.

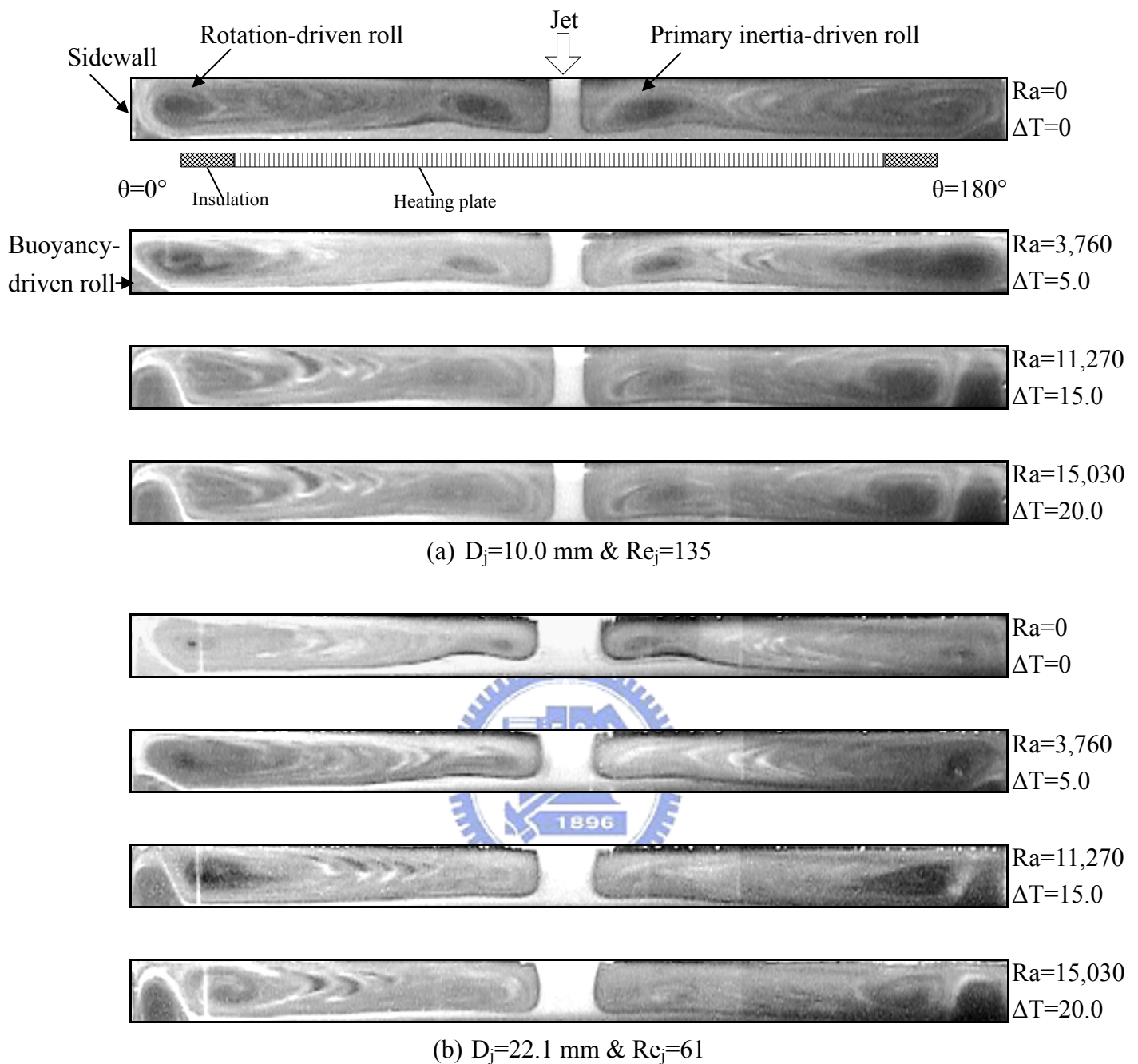


Fig. 4.25 Steady side view flow photos taken at the cross plane $\theta = 0^\circ$ & 180° for various Rayleigh numbers at $Q_j = 1.0 \text{ slpm}$ and $Re_\Omega = 1,557$ ($\Omega = 20 \text{ rpm}$) for (a) $D_j = 10.0 \text{ mm}$ & $Re_j = 135$ and (b) $D_j = 22.1 \text{ mm}$ & $Re_j = 61$.

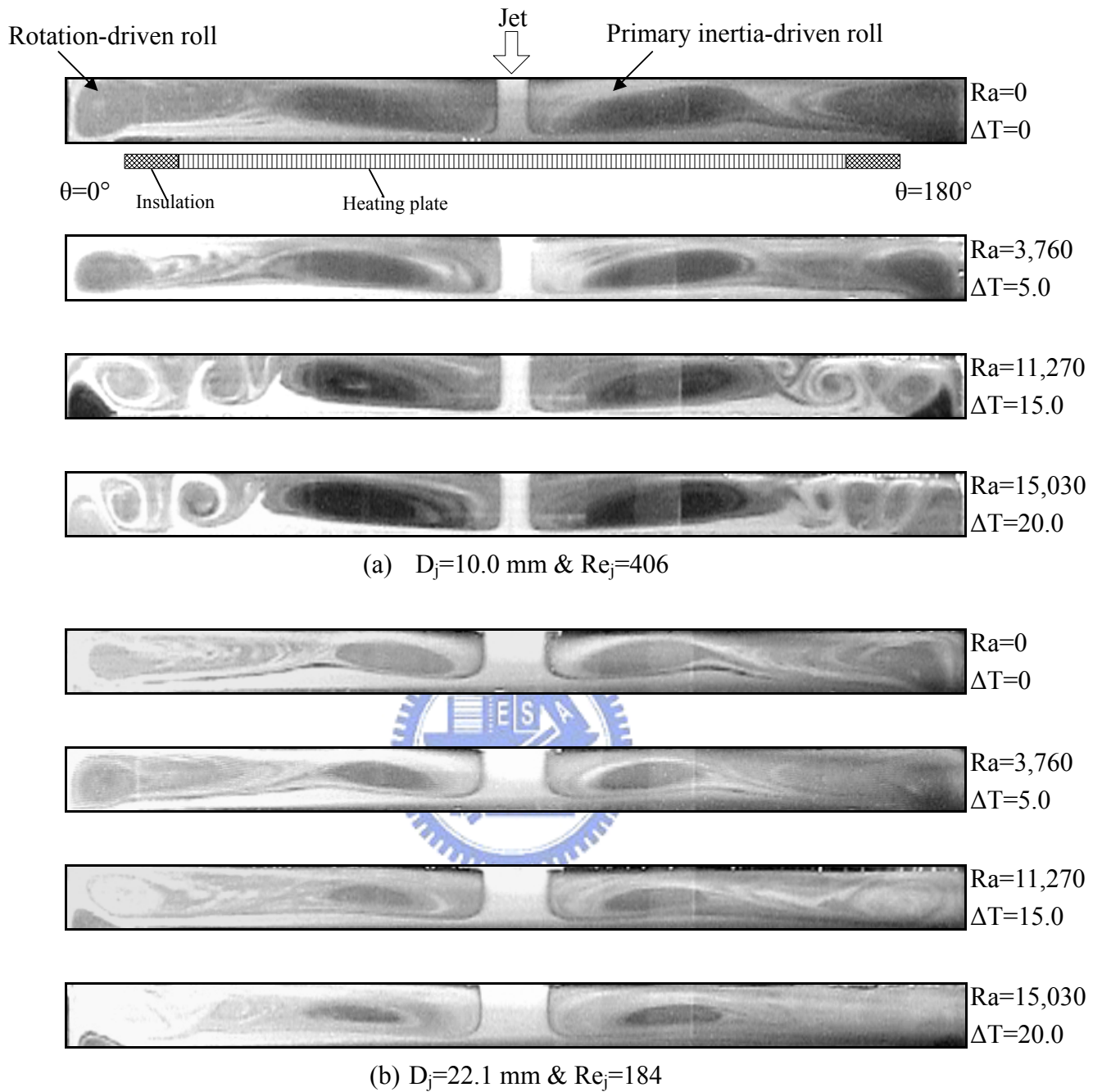


Fig. 4.26 Side view flow photos taken at the cross plane $\theta = 0^\circ$ & 180° for various Rayleigh numbers at $Q_j = 3.0$ slpm and $Re_\Omega = 1,557$ ($\Omega = 20$ rpm) for (a) $D_j = 10.0$ mm & $Re_j = 406$ and (b) $D_j = 22.1$ mm & $Re_j = 184$.

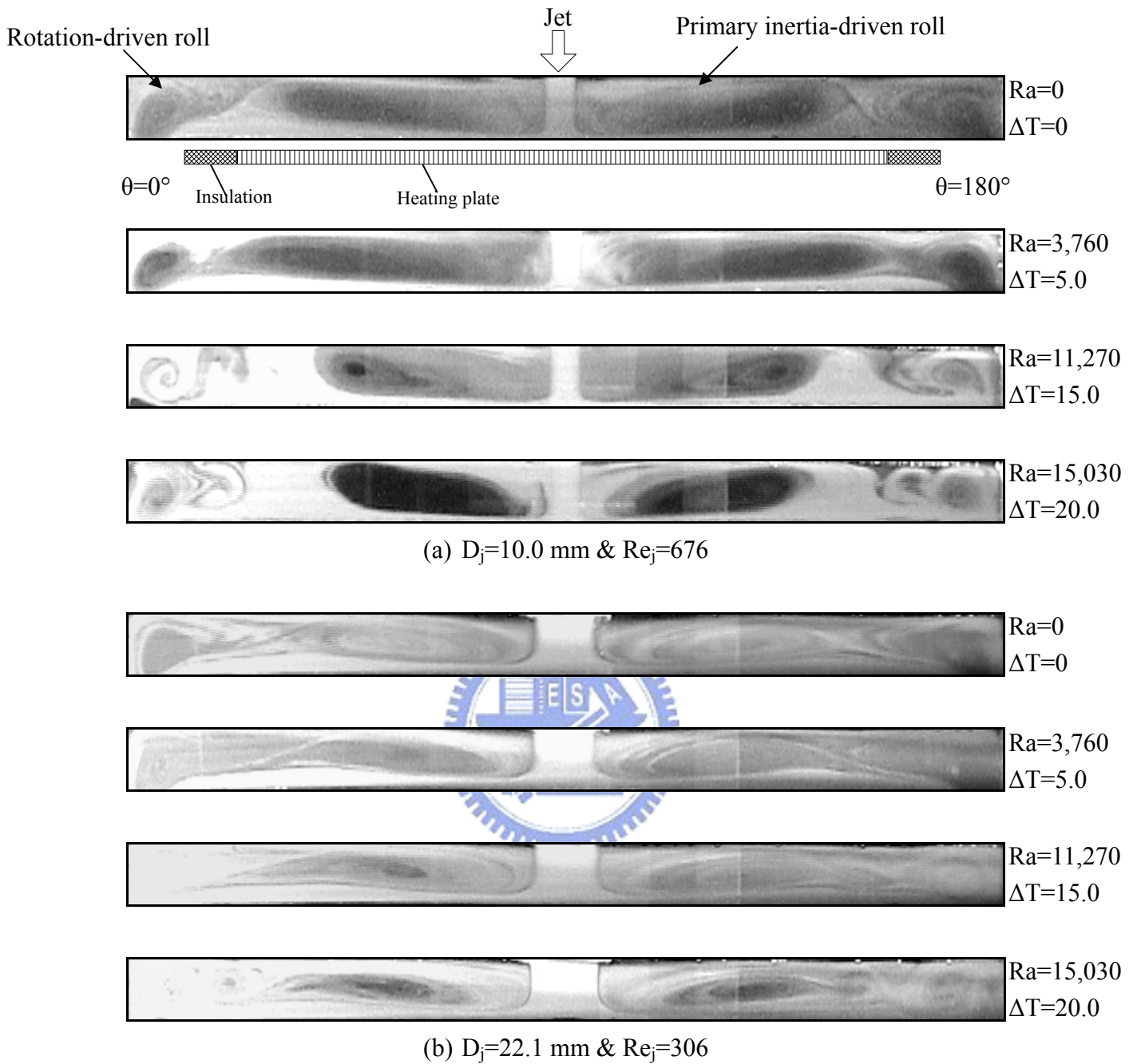


Fig. 4.27 Side view flow photos taken at the cross plane $\theta = 0^\circ$ & 180° for various Rayleigh numbers at $Q_j = 5.0 \text{ slpm}$ and $Re_\Omega = 1,557$ ($\Omega = 20 \text{ rpm}$) for (a) $D_j = 10.0 \text{ mm}$ & $Re_j = 676$ and (b) $D_j = 22.1 \text{ mm}$ & $Re_j = 306$.